

Numerical processing of thin-film sensor temperature data

L. Battisti¹, E. Bertolazzi¹ & F. Trivellato²

¹*Department of Mechanical and Structures Engineering,*

²*Department of Civil and Environmental Engineering, University of Trento, Italy*

Abstract

A thin-film sensor operating in transient mode in principle enables very accurate temperature measurements to be obtained, e. g. in turbine blades, because of the high frequency of its response; however, the complexity of data processing is the major drawback for popular use of the sensor.

In this study new data processing methods are presented, including a comprehensive 1-D finite element model which is convenient both for its capability of dealing with general boundary conditions and for the low computational cost as compared to present transform-based methods.

This method can also tackle single-, double- and multi-layer sensors, can support temperature dependent quantities and proves successful in processing prototype signals in a wide range of Mach numbers. A new procedure is also proposed, which is useful for the design of an experiment on a rational basis.

1 Introduction

The assessment of heat fluxes is of relevance in studying high temperature components of power and gas turbine engineering; the thin-film resistance thermometer is one of the most common fast-response sensors.

The solution of the 1-D heat conduction equation is typically obtained by means of either electric analogy or numerical integration [1]. The analysis of the analog signal needs digital processing for low frequency signals; it can neither account for variable properties of the substrate nor for fluctuating heat transfers. A comprehensive evaluation of existing methodologies is presented in [2], which is the closest work to the present paper.



Both analog and numerical approaches which have been proposed so far share a number of limitations, namely: (i) analog hardwares require bandwidths that must increase according to sampling rates; (ii) temperature dependent quantities of substrates cannot be modeled; (iii) measurements are affected by the semi-infinite slab assumption; and (iv) the solution is computationally expensive in the double layer sensor, while it is difficult to obtain at all if the number of substrates is greater than two.

Data processing by means of efficient numerical tools is the focus of this paper; all the analytical and numerical formulations hereinafter illustrated are fully detailed in [3].

2 Statement of the problem

It is assumed in this study that only convective and conductive heat fluxes are relevant to the phenomenon under investigation, while other heat sources may be neglected, [4].

Considering a slab composed of m different layers, whose total thickness is ℓ , the temperature distribution within the slab is described by the following set of m heat conduction equations:

$$\frac{\partial}{\partial t} \left(\rho_i(\Theta) c_i(\Theta) \Theta \right) = \frac{\partial}{\partial z} \left(\lambda_i(\Theta) \frac{\partial \Theta}{\partial z} \right), \quad z_{i-1} < z < z_i, \quad i = 1, \dots, m \quad (1)$$

where $\Theta = \Theta(t, z)$ is a piecewise continuous C^1 function; z_i are the boundaries of the layers; $z_0 = 0$ and $z_m = \ell$; ρ , c and λ are respectively the mass density, the heat capacity and the thermal conductivity of the slab.

The above set of 1-D parabolic equations are coupled to the following $m - 1$ interface conditions:

$$\lim_{z \rightarrow z_i^-} \lambda_i(\Theta) \frac{\partial \Theta}{\partial z} = \lim_{z \rightarrow z_i^+} \lambda_{i+1}(\Theta) \frac{\partial \Theta}{\partial z}, \quad i = 1, 2, \dots, m - 1 \quad (2)$$

The upper heat flux, $\dot{q}_s(t)$, and the lower heat flux, $\dot{q}_b(t)$, are defined as follows:

$$\dot{q}_s(t) = -\lambda_1(\Theta(t, 0)) \frac{\partial \Theta}{\partial z} \Big|_{z=0}, \quad \dot{q}_b(t) = -\lambda_m(\Theta(t, \ell)) \frac{\partial \Theta}{\partial z} \Big|_{z=\ell}. \quad (3)$$

The set of governing equations is closed by:

- (i) the initial condition: $\Theta(0, z) = \Theta^{init}(z)$, for $0 \leq z \leq \ell$;
- (ii) the top boundary condition: $\Theta(t, 0) = \Theta^s(t)$, for $z = 0$;
- (iii) the bottom boundary condition: $\Theta(t, \ell) = \Theta^\ell(t)$, for $z = \ell$.

As the signal $\Theta^s(t)$ is known by measurements, the temperature $\Theta(t, z)$ is obtained by eqns.(1). In simple cases the temperature $\Theta(t, z)$ can be computed exactly; otherwise it must be calculated by numerical techniques. The heat flux $\dot{q}_s(t)$ is then deduced by eqn.(3).



3 Single and double layer slab

The 1-D semi-infinite slab is modeled with $\ell = \infty$ and $m = 1$ ($m = 2$ in the double layer case); the slab is assumed to be in thermal equilibrium at time $t = 0$ so that, without loss of generality, $\Theta(0, z) = 0, \forall z \geq 0$. If the quantities ρ, c and λ within each layer are regarded as constants, with the value of the constants known at the initial temperature, then eqns.(1) can be solved by means of the Laplace's transform. According to the Heaviside approximation, the heat signal $\dot{q}_s(t)$ increases in the rise time t_H , then it drops down roughly linearly. The absolute error for the heat signal is, [3]:

$$|E(t)| \leq M_1 \sqrt{\frac{t_H}{t}} + M_2 \quad (4)$$

The constant M_1 is of the order of the maximum heat flux, while the constant M_2 is controlled by heat fluctuations after the rise time. Eqn.(4) is a useful guideline to evaluate the appropriate time duration of measurement.

4 A new implicit method

The CF (Cook and Felderman) method, [1], is based on a piecewise linear approximation of $\Theta(t, 0)$. A new implicit version of the CF method can be derived by introducing the piecewise constant spline $\dot{q}^L(t)$:

$$\dot{q}^L(\tau) = \dot{q}_{s_{j-1/2}}, \quad t_{j-1} \leq \tau \leq t_j \quad . \quad (5)$$

An implicit linear relation in the unknowns $\dot{q}_{s_{j-1/2}}$ is then obtained, [3].

5 Multi-layer slab

Not only the methods based on the Laplace's transform are difficult to implement in multi-layer sensors, but also they are extremely costly even only in the double layer case.

Multiplying eqns.(1) by the test function $\Phi(z)$, integrating by parts on the interval $[0, \ell]$, taking advantage of eqns.(2), it can be obtained, [3]:

$$\begin{aligned} & \int_0^\ell \left(\rho(z, \Theta) c(z, \Theta) \Phi(z) \frac{\partial \Theta}{\partial t} + \lambda(z, \Theta) \Phi'(z) \frac{\partial \Theta}{\partial z} \right) dz = \\ & = \Phi(\ell) \lambda(\ell, \Theta(t, \ell)) \frac{\partial \Theta}{\partial z} \Big|_{z=\ell} - \Phi(0) \lambda(0, \Theta(t, 0)) \frac{\partial \Theta}{\partial z} \Big|_{z=0} \end{aligned} \quad (6)$$

The solution $\Theta(t, z)$ of the problem is the function that satisfies eqn.(6) for all the test functions Φ . The structure of eqn.(6) suggests the Finite Element (FE) method as the most natural approximation. This widely known numerical method is based



on the approximation of the solution in a finite dimensional subspace; using the FE method the following set of ordinary differential equations may be derived:

$$\sum_{i=0}^n \Theta_i'(t) A_{i,k}(\Theta) + \sum_{i=0}^n \Theta_i(t) B_{i,k}(\Theta) = 0, \quad k = 1, 2, \dots, n$$

where $\Theta_0(t) = \Theta^*(t)$. The coefficients $A_{i,k}(\Theta)$ and $B_{i,k}(\Theta)$ have been calculated by the trapezoidal rule; A semi-implicit time integration scheme, based on a modified version of the implicit Euler scheme, turned out to be both stable and computationally cheap. A strictly diagonally dominant tridiagonal system with positive elements on the diagonal and non negative elements elsewhere has to be solved. The system matrix is an M-matrix, [5]; its solution satisfies the discrete maximum principle, [6], and therefore the FE method is unconditionally stable.

6 The design of an experiment

Defining $\Delta t = 1/f_s$, where f_s is the sampling frequency, Δz = the maximum length of FE intervals, the asymptotic total error E_T for $\Delta t, \Delta z \mapsto 0$ is derived as:

$$E_T \approx E_S \Delta t + E_M \Delta z^2 \quad (7)$$

where E_S and E_M are unknown constants. The total error turns out to be controlled by two contributions: (i) the temporal sampling error $E_S \Delta t$, which is controlled by acquisition hardwares (however, the sampling error is often smaller than the error due to parameter uncertainties, e.g. the values of physical properties claimed by manufacturers); (ii) the spatial sampling error $E_M \Delta z^2$, due to mesh discretization.

The parameter

$$P = \frac{E_S}{E_M} \frac{\Delta t}{\Delta z^2} \quad (8)$$

is here introduced to optimize the spatial discretization with respect to sampling frequency; whenever $P \gg 1$ the error is dominated by a small sampling rate or by an excessive fine mesh. Otherwise, if $P \ll 1$, the error is dominated by too great a sampling rate or by a coarse mesh. When facing the design of an experiment, it is clear that mesh discretization must be tuned according to available accuracy; imposing $P \approx 1$, the mesh size may be chosen according to the following guideline:

$$\Delta z \approx \sqrt{\frac{E_S}{E_M} \frac{1}{f_s}} \propto f_s^{-1/2} \quad (9)$$

Also, from eqns.(7) and (8), it follows that:

$$E_T \approx \frac{E_S}{f_s} \left(1 + \frac{1}{P} \right)$$

Keeping $\Delta z \propto f_s^{-1/2}$, the parameter P remains nearly constant, so that when the sampling frequency goes to infinity, the total error goes to 0. The computational



Table 1: Validation tests of the numerical methods.

test #	layer	$S [W/m^2]$	$B [W/m^2]$	$f_q [Hz]$	$f_s [Hz]$
1	single	1000	0	0	10
2	single	1000	0	0	100
3	single	1000	0	0	1000
4	single	1000	500	4	10
5	single	1000	500	4	100
6	single	1000	500	4	1000
7	double	1000	0	0	10
8	double	1000	0	0	100
9	double	1000	0	0	1000
10	double	1000	500	4	10
11	double	1000	500	4	100
12	double	1000	500	4	1000

Table 2: Raw (not filtered) prototype data.

test #	Mach	f_s (Hz)	Layer	Facility	Refer.
13	0.02	500	double	Trento University, Italy	[7]
14	0.60	250	single	v.Karman Inst., Belgium	[8]
15	6.00	250	single	v.Karman Inst., Belgium	[9]
16	6.00	25	single	v.Karman Inst., Belgium	[9]

cost is $\mathcal{O}(n_s^{3/2})$, while the accuracy is $\mathcal{O}(n_s^{-2})$, where n_s = number of temperature data. The overall performance of the FE method is therefore remarkable, also because the computational time is $\mathcal{O}(10\text{ s})$ in a typical laptop computer for $n_s \simeq 10^6$. It is also worth mentioning the easy treatment of non linear cases, which is one of the most notable features of FE method. The same is not true for transform-based methods.

7 Results

7.1 Code validation

An ideal signal has been used for a semi-infinite slab having constant physical properties: $\dot{q}_s(t) = S + B \cos(2\pi f_q t + \phi)$, where S is the step magnitude; B ,



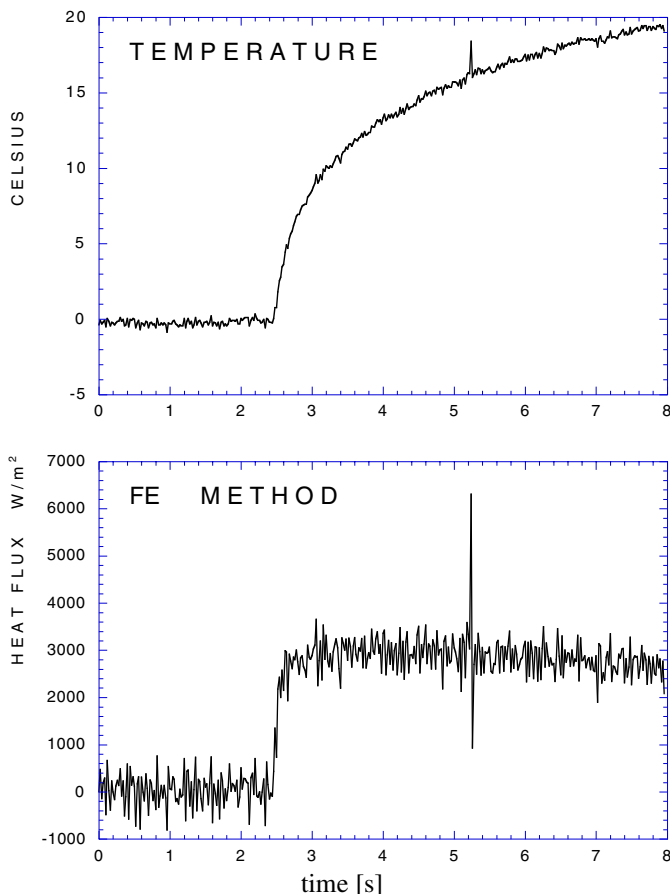


Figure 1: Heat flux reconstruction in W/m^2 (test #13, $f_s = 500\text{ Hz}$).

f_q and ϕ are respectively the magnitude, frequency and phase of the superimposed signal.

Table 1 illustrates 12 tests that have been performed to compare the above presented numerical methods – i.e. the new implicit method and the FE scheme – with the standard CF method. The comparison among the methods, not reported here for brevity's sake, is described at length in [3]. In test #4 the signal reconstruction is poor for all of the methods, while at higher f_s values (tests #5 and 6) the simulation of the signal is remarkable. The FE method turned out to be computationally cheaper and more precise than the standard CF method. Both tests #4 and 10 pointed to a threshold value $f_s/f_q \approx 2.5$, below which the signal reconstruction is not satisfactory. This was also demonstrated by tests #5, 6, 11 and 12, where higher frequency ratios are successful in retrieving the heat signal.



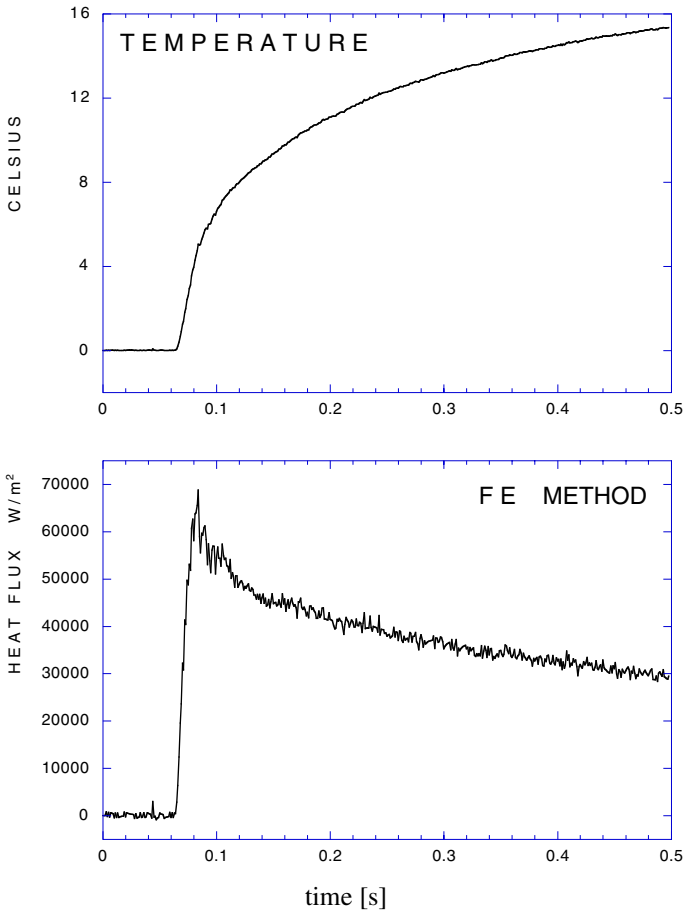


Figure 2: Heat flux reconstruction in W/m^2 (test #14, $f_s = 250\text{ Hz}$).

7.2 Processing of raw (not filtered) prototype data

Raw experimental data which have been collected in prototype facilities have also been used to compare the presented methods. Figs.1, 2 and 3 illustrate typical temperature time histories and heat flux reconstructions for tests #13,14 and 15 (see table 2) by the FE method; even though reconstructions worked well for all of the methods, the CF method and the new implicit method do require the longest CPU times.

Fig.3–c shows the heat flux reconstruction if a sampling rate of 25 Hz is used instead of 250 Hz (fig.3–b). It seems there is no need to sample at the demanding frequency of 250 Hz , as no apparent loss of information occurs when sampling at a more comfortable frequency, which can be as low as 25 Hz . This result is of relevance when facing the design of an experiment. When lower surface tempera-



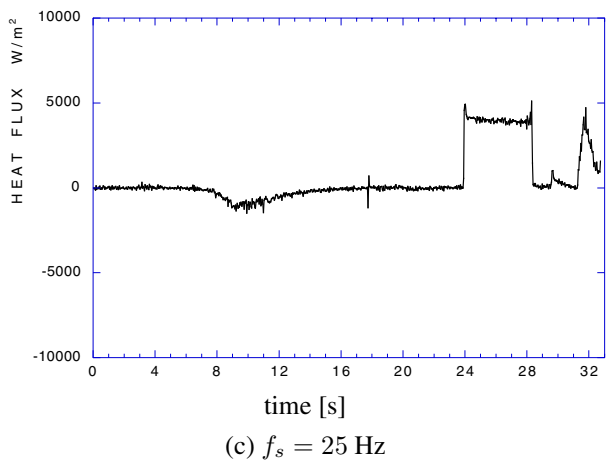
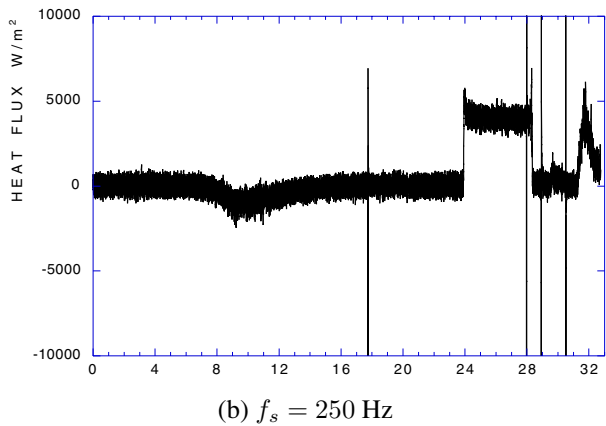
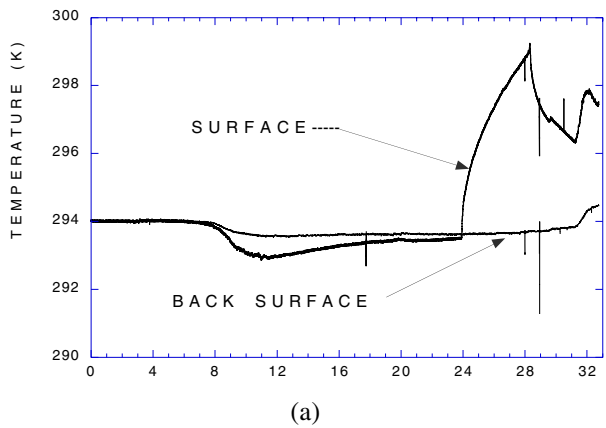


Figure 3: Heat flux in W/m^2 (test #15; FE method).

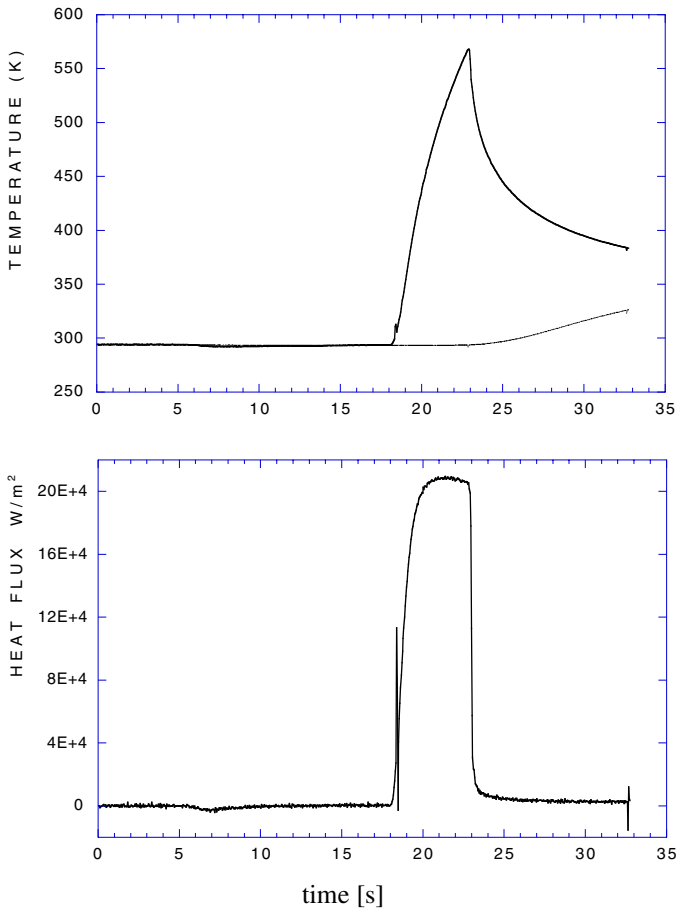


Figure 4: Heat flux in W/m^2 (test #16; FE method).

tures of the substrate do change meaningfully, the semi-infinite assumption is no longer valid and both the standard CF and the implicit method cannot be used at all; moreover, if the top surface does experience abrupt temperature gradients, the assumption of constant physical properties can affect the solution accuracy. In this latter case, the FE method *must* be used and a typical example is presented in fig.4, where time histories of top and back surface temperatures of a model are plotted on the top diagram. Fig.4 shows the heat flux as calculated by the FE method with constant physical properties; there is basically no difference with the results elaborated by [9]. When variable properties are taken into account, it turns out that the maximum difference between the two solutions is definitely small (roughly 2.5%).



8 Conclusions

The standard CF method has been improved in this study by an implicit version. A comprehensive FE method has also been implemented that proved successful in reconstructing signals of known test functions: in addition experimental and *not filtered* data have been accurately processed. The influence of the variability of physical properties on the accuracy of the solution has also been addressed. Results do confirm the performance of the FE code which is capable of reconstructing signals even at very low sampling frequencies. The computational cost of the FE method proved enormously lower than that of any other former technique of literature; if the semi-infinite slab assumption is no longer valid (e.g., leading edge of turbine blades) the FE approach is the only feasible. A guideline useful to minimize *a priori* the experimental error has been proposed.

Acknowledgements

L. Battisti is grateful to Prof. T. Arts and Prof. J. M. Charbonnier (von Karman Institute, Belgium) for useful discussions. He acknowledges the staff of the Laboratory of Turbomachinery and Aeronautics (von Karman Institute, Belgium) for the assistance in performing tests #14,15 and 16.

References

- [1] Cook, W.J. & Felderman, E.J., Reduction of data from thin film heat transfer gauges: A concise numerical technique. *AIAA Journal*, (4), No.3, pp.561–562, 1966.
- [2] Walker, D.G. & Scott, E.P., Evaluation of estimation methods for high unsteady heat fluxes from surface measurements, *J. of Thermophysics and Heat Transfer*, (12), pp. 543–551, 1998.
- [3] Battisti, L. & Bertolazzi, E., Thin film heat transfer data reduction by means of some numerical techniques, Tech. Rep. #15, Dept. of Mechanical and Structures Engineering, Trento University, Italy, 2001.
- [4] Battisti, L. & Charbonnier, J.M., Transient radiant heat transfer measurements technique on hot surface model. Tech. Rep. #15, VKI–NATO–CNR Research Project, March 2000.
- [5] Axelsson, O., *Iterative Solution Methods*. Cambridge Univ. Press, 1994.
- [6] Bertolazzi, E., Numerical conservation and discrete maximum principle for elliptic pdes. *Mathematical Models and Methods in Applied Sciences*, (8), pp. 685–711, 1998.
- [7] Battisti, L. & Schmeer, T., Experimental study of the surface heat transfer enhancement in a rib roughened blade coolant channel by means of double layer thin films. *Proceedings, 55^o Eurotherm Seminar*, Santorini, Greece, 1997.
- [8] Pelle, O. & Arts, T., Development of a double layer thin film gauge for surface



- heat transfer measurement. *Proceedings, 55^o Eurotherm Seminar*, Santorini, Greece, 1997.
- [9] Marquet, B. & Charbonnier, J.M., Shock wave boundary layer interaction on hot surfaces: Pressure and heat transfer measurements on hot wall compression ramp models at Mach 6. Technical Note GSTP1-TR-6301-VKIN, 1998.

